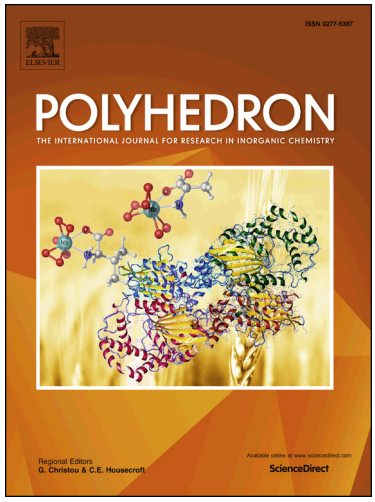

Bis-substituted diphenylamine arylidene hydrazones for the synthesis of new binuclear organotin(IV) complexes: crystal structure, DNA cleavage and molecular docking

Maryam Yousefi, Tahereh Sedaghat, Jim Simpson, Hossein Motamedi, Mohammad Reza Dayer

PII: S0277-5387(18)30506-0
DOI: https://doi.org/10.1016/j.poly.2018.08.040
Reference: POLY 13363

To appear in: *Polyhedron*

Received Date: 25 June 2018
Revised Date: 27 July 2018
Accepted Date: 10 August 2018

Please cite this article as: M. Yousefi, T. Sedaghat, J. Simpson, H. Motamedi, M.R. Dayer, Bis-substituted diphenylamine arylidene hydrazones for the synthesis of new binuclear organotin(IV) complexes: crystal structure, DNA cleavage and molecular docking, *Polyhedron* (2018), doi: https://doi.org/10.1016/j.poly.2018.08.040

Bis-substituted diphenylamine arylidene hydrazones for the synthesis of new binuclear organotin(IV) complexes: crystal structure, DNA cleavage and molecular docking

Maryam Yousefi[a], Tahereh Sedaghat[a,*], Jim Simpson[b], Hossein Motamedi [c,d], Mohammad Reza Dayer[c]

[a] *Department of Chemistry, Faculty of Science, Shahid Chamran University of Ahvaz, Ahvaz, Iran*

[b] *Department of Chemistry, University of Otago, PO Box 56, Dunedin 9054, New Zealand*

[c]*Department of Biology, Faculty of Sciences, Shahid Chamran University of Ahvaz, Ahvaz, Iran*

[d]*Biotechnology and Biological Science Research Center, Shahid Chamran University of Ahvaz, Ahvaz, Iran*

**corresponding author: tsedaghat@scu.ac.ir*

Abstract

Five dinuclear organotin(IV) complexes, $R_4Sn_2L^a$ (R = Me, Ph) and $R_4Sn_2L^b$ (R = Me, Ph and Bu) have been synthesized from reaction of R_2SnCl_2 with 2, 4′- and 2, 2′-bis-substituted diphenylamine arylidene hydrazones, H_4L^a and H_4L^b, respectively. The synthesized compounds have been investigated by elemental analysis and IR, ^{1}H NMR, and ^{119}Sn NMR spectroscopy. The structures of $Me_4Sn_2L^b$ and $Ph_4Sn_2L^b$ have been also confirmed by X-ray crystallography. The results show that the fully deprotonated bis-hydrazone ligand provides two contiguous ONO tridentate domains that coordinate to the two SnR_2 moieties in the enolate form. Each tin atom in the complexes adopts a five-coordinate environment. Ligands and complexes showed no antibacterial activity against Gram-positive (*Bacillus subtilis* and *Staphylococcus aureus*) and Gram-negative (*Escherichia coli* and *Pseudomonas aeruginosa*) bacteria. However, both ligands and their methyl complexes were found to degrade DNA, an observation that adapt with the mode of interaction suggested by molecular docking.

Keywords: organotin(IV); hydrazone; crystal structure; ^{119}Sn NMR; DNA cleavage, molecular docking

1.Introduction

Interest in the use of acyl-/aroyl-dihydrazones as polyfunctional ligands has increased considerably [1-5]. Such ligands are derived from the condensation of acyl-/aroyl-dihydrazines (organic acid dihydrazides) with aldehydes or ketones. The presence of two coordinating units with several binding sites connected by bridges with different degrees of flexibility may produce better coordinating properties in these ligands than for ligands with a single coordinating unit. They are able to create different supramolecular architectures, coordination polymers and polynuclear complexes involving ligand bridging [6-10]. Binuclear complexes of bis-hydrazones may also be able to mimic the bimetallic sites found in several enzymes. To date the structure of many transition metal complexes of multidentate dihydrazones have been studied extensively [1, 4, 11, 12]. However, a survey of literature reveals that the binuclear organotin(IV) complexes with these types of ligands have been less widely studied. Research into the organotin chemistry is a prolific area of chemical investigations. These compounds have found more industrial, agricultural and medicinal applications than any other organometallic compounds [13-16]. In addition, they present an interesting structural variety, so that structural studies have always been prominent in organotin(IV) chemistry [13, 14, 17]. Among these investigations, hydrazone organotin(IV) complexes have received much attention because of their potential pharmacological applications and the possibility of chemical variations due to the presence of different functional groups [18-23]. Because of this, the inclusion of two organotin units, instead of just one, in the same molecular entity may produce new compounds with interesting biological and structural properties. In this line, the first binuclear organotin(IV) complexes of dihydrazones were synthesized in 1994 by Gopinathan and coworkers [24]. Then, in 2008, Yin et al. reported dinuclear organotin(IV) complexes of bis-aroyl-hydrazones with a rigid spacer

between the hydrazine units [25]. Recently, the synthesis and structural investigation of binuclear organotin complexes of bis-hydrazones have received attention again and we have also published several articles in this area [26-34]. In most of these complexes, the dihydrazone ligand was symmetric and both tin atoms were in the same chemical environments. This is readily proven by observing only one signal in ^{119}Sn NMR spectrum of the resulting complex. Recently we have also reported binuclear organotin complexes of a multiprotic dihydrazone ligand containing both ONS and ONN tridentate donor environments [33]. In a continuation of our research into symmetric and asymmetric binuclear organotin complexes of bis-hydrazones, in this study we have used diphenylamine as a linker for the synthesis of new types of dinuclear Sn(IV) complexes with the N-aryl anthranilic acid ligands. It has been shown previously that diphenylamine derivatives are anticancer and orally active antiproliferative agents that inhibit tyrosine kinase autophosphorylation. Anti-inflammatory activity is also exhibited by a variety of N-aryl anthranilic acid derivatives [35-37]. In view of the likely structural diversity and potential anticancer activity of organotin(IV) complexes of such hydrazones, we report here the synthesis of 2, 4′- and the more symmetrical 2, 2′-bis-substituted diphenylamine arylidene hydrazones, Figure 1, and their use as binucleating ligands for the synthesis of a series of organotin(IV) complexes.

2. Experimental

2.1. Materials and methods

All starting materials were obtained from commercial suppliers and used as received without further purification. Copper powder used as catalyst for the synthesis of diphenylamine carboxylic acids was activated by washing with a 1: l mixture of acetone and concentrated HCl

and then with aqueous acetone, and dried in a vacuum oven. 2, 4′-diphenylamine dicarboxylic acid (**3a**) was prepared according to a literature method with some modifications from the reaction of 2-chlorobenzoic acid (**1**) and 4-aminobenzoic acid, **2a,** in the presence of the copper catalyst and excess potassium carbonate by refluxing for 18 h in DMF (m.p. 288 °C) [38]. 2-[4-(methoxycarbonyl)phenylamino] benzoic acid methyl ester (m.p. 75 °C) (**4a**) and 2-[4-(hydrazinecarbonyl)phenylamino] benzoic acid hydrazide (m.p. 245 °C) (**5a**) were also prepared by reported procedures with an increase in the reflux time [36].

The IR spectra were obtained using an FT BOMEM MB102 spectrophotometer. The ^{1}H and ^{119}Sn NMR spectra were recorded with a Bruker Avance Ultrashield spectrometer using TMS and $SnMe_4$ respectively as internal references. Melting points were determined on a Thermo Scientific LTD IA9200 apparatus. Elemental analyses were carried out on an Elementar vario EL III analyzer.

*2.2. Synthesis of H_4L^a (**6a**)*

2-[4-(Hydrazinecarbonyl)phenylamino]benzoic acid hydrazide (**5a,** 0.304 g, 1.2 mmol) and 2-hydroxynaphthaldehyde (0.413 g, 2.4 mmol) were dissolved in ethanol (10 mL). Then two drops of glacial acetic acid were added and the solution was refluxed for 6 h. The resulting green-yellow precipitate was filtered and washed with ethanol. Yield: 0.611 g (86%); m.p. 298 °C Anal. Calcd. for $C_{36}H_{27}N_5O_4$: C, 72.84; H, 4.58; N, 11.80 %. Found: C, 72.98; H, 4.73; N, 11.68 %. FT-IR (KBr, cm^{-1}): ν(N–H), 3366, 3219, ν(Ar–H), 3056; ν(C=O), 1640; ν(C=N), 1620. ^{1}H NMR (250 MHz, DMSO-d_6): δ = 12.90, 12.70 (s, 2H, $H_{b,b'}$), 12.27, 12.07 (s, 2H, $H_{c,c'}$), 9.52 (s, 1H, NH), 9.46, 9.44 (s, 2H, $H_{a,a'}$), 8.26-7.09 (m, 20H, Ar-H).

*2.3. Synthesis of [$Me_4Sn_2L^a$] (**7a**)*

To a stirred solution of H_4L^a (0.148 g, 0.25 mmol) in ethanol (5 mL) triethylamine (1 mmol) was added. This suspension was stirred for 10 min and then Me_2SnCl_2 (0.109 g, 0.5 mmol) in ethanol (5 mL) was added. The suspension was refluxed for 4 h and during which time the yellow precipitate changed to an orange solid product. This precipitate was collected, washed with ethanol (5 mL) and dried in vacuum over $CaCl_2$. Yield: 0.20 g (90%); m.p. 240 °C. Anal. Calcd. for $C_{40}H_{35}N_5O_4Sn_2$: C, 54.15; H, 3.98 N, 7.89 %. Found: C, 54.53; H, 3.82; N, 7.87 %. FT-IR (KBr, cm^{-1}): ν(C=N), 1616, 1601; ν_{as}(Sn–C), 656; ν_s(Sn–C), 562; ν(Sn–O), 523; ν(Sn–N), 464. ^{1}H NMR (250 MHz, DMSO-d_6): δ = 10.48 (s, 1H, NH), 9.70, 9.57 (s, 2H, $H_{a,a'}$, $^3J(^{119}Sn\text{-}^1H)$ = 32.4 Hz), 8.31-6.90 (m, 20H, Ar-H), 0.77, 0.74 [s, 12H, Me_2Sn, $^2J(^{119}Sn\text{-}^1H)$ = 88.3 Hz]. ^{119}Sn NMR (186 MHz, DMSO): δ = –208.2, –233.6.

*2.4. Synthesis of [$Ph_4Sn_2L^a$] (**8a**)*

Complex **8a** was synthesized as described for **7a** from H_4L^a (0.148 g, 0.25 mmol), triethylamine (0.13 mL, 1 mmol) and Ph_2SnCl_2 (0.172 g, 0.0.5 mmol). Yield: 0.22 g (78%); m.p. 272 °C; Anal. Calcd. for $C_{60}H_{43}N_5O_4Sn_2$: C, 63.47; H, 3.82; N, 6.17 %. Found: C, 63.76; H, 4.23; N, 6.21 %. FT-IR (KBr, cm^{-1}): ν(C=N), 1616, 1600; ν(Sn–O), 505; ν(Sn–N), 440. ^{1}H NMR (250 MHz, DMSO-d_6): δ = 10.55 (s, 1H, NH), 9.75, 9.58 (s, 2H, $H_{a,a'}$, $^3J(^{119}Sn\text{-}^1H)$ = 29.8 Hz), 8.38–7.00 (m, 40H, Ar-H), ^{119}Sn NMR (186 MHz, DMSO): δ = –399.6, –420.4.

*2.5. Synthesis of 2, 2′-diphenylamine dicarboxylic acid (**3b**)*

This compound was synthesized by a procedure similar to that used for **3a**. A solution of 2-chlorobenzoic acid (**1**, 5.16 g, 33 mmol) and potassium carbonate (15 g, 180 mmol) in DMF (40

mL) was stirred for 15 min. Then a mixture of 2-aminobenzoic acid (**2b**, 4.93 g, 36 mmol) and copper powder (0.6 g) in DMF (40 mL) was added. This mixture was refluxed for 20 h, at 140-145 °C and under a stream of nitrogen gas. During this time the color of the mixture changed from brown to pink. The mixture was cooled to 60 °C, added to 200 mL of ice-water and stirred for 15 min. This solution was decolorized using activated carbon (3 g) at 100 °C with stirring for 10 min. The mixture was filtered and enough HCl (6 M) was added to the solution in an ice bath until the formation of precipitation was completed. The yellow solid product was filtered, washed with water and dried at 50 °C in an oven. Yield: 6.62 g (78%); m.p. 293 °C; FT-IR (KBr, cm^{-1}): ν(N–H), 3330 sh; ν(O–H), 3000-2800 br; ν(C=O), 1667. ^{1}H NMR (300 MHz, DMSO-d_6): δ = 13.01 (s, 2H, OH), 10.81(s, 1H, NH), 7.91-6.91 (m, 8H, Ar-H).

*2.6. Synthesis of 2-[2-(methoxycarbonyl)phenylamino] benzoic acid methyl ester (**4b**)*

This compound was synthesized by a similar procedure to that reported for the chloro-derivative of this compound with some modifications [37]. To a stirred solution of **3b** (6.20 g, 24.12 mmol) in MeOH (124 mL) in an ice bath, thionyl chloride (6.1 mL) was added dropwise. This solution was stirred for 20 min at room temperature and then refluxed for 12 h. The dark solution was then concentrated to half volume and put aside. The resulting pale green crystals were collected and dried. Yield: 6.4 g (98%); m.p. 92 °C; FT-IR (KBr, cm^{-1}): ν(N–H), 3309 sh; ν(C–$H_{aliphatic}$), 2985-2940; ν(C=O), 1700. ^{1}H NMR (300 MHz, DMSO-d_6): δ = 10.72(s, 1H, NH), 7.92-6.95 (m, 8H, Ar-H), 3.85 (s, 6H, CH_3).

2.7. Synthesis of 2-[2-(hydrazinecarbonyl)phenylamino]benzoic acid hydrazide (**5b**)

Hydrazine hydrate (64 mL) was added to **4b** (6.7 g, 23.6 mmol) and the solution was refluxed for 15 h. The resulting white solid was filtered and dried. Yield: 6.2 g (95%); m.p. 275 °C; FT-IR (KBr, cm^{-1}): ν(N–H), 3360, 3278, 3172; ν(C=O), 1645. ^{1}H NMR (300 MHz, DMSO-d_6): δ = 10.22 (s, 1H, NH), 9.64 (s, 2H, NH), 7.48-6.84 (m, 8H, Ar-H), 4.44 (s, 4H, NH_2).

*2.8. Synthesis of H_4L^b (**6b**)*

A solution of 2-hydroxynaphthaldehyde (0.413 g, 2.4 mmol) and **5b** (0.317 g, 1.2 mmol) in EtOH (10 mL) was refluxed for 6 h. The green-yellow solid product was filtered and washed with EtOH. Yield: 0.572 g (83%); m.p. 275 °C; Anal. Calcd. for $C_{36}H_{27}N_5O_4$: C, 72.84; H, 4.58; N, 11.80 %. Found: C, 72.73; H, 4.43; N, 11.95%. FT-IR (KBr, cm^{-1}): ν(N–H), 3360, 3241, ν(Ar–H), 3060; ν(C=O), 1638; ν(C=N), 1624. ^{1}H NMR (300 MHz, DMSO-d_6): δ = 12.73 (s, 2H, OH), 12.20 (s, 2H, NH), 10.32 (s, 1H, NH), 9.42 (s, 2H, CH=N), 8.21-7.06 (m, 20H, Ar-H).

*2.9. Synthesis of [$Me_4Sn_2L^b$] (**7b**)*

Complex **7b** was synthesized as described for **7a** from H_4L^b (0.148 g, 0.25 mmol), triethylamine (1 mmol) and Me_2SnCl_2 (0.109 g, 0.5 mmol) after a 6 h reflux. Yellow block-like crystals suitable for X-ray crystallography were obtained by slow evaporation of an ethanol/methanol (2:1) solution. Yield: 0.22 g (99%); m.p. 250 °C; Anal. Calcd. for $C_{40}H_{35}N_5O_4Sn_2$: C, 54.15; H, 3.98 N, 7.89 %. Found: C, 54.29; H, 3.91; N, 7.93 %. FT-IR (KBr, cm^{-1}): ν(C=N), 1617, 1600; ν_{as}(Sn–C), 649; ν_s(Sn–C), 562; ν(Sn–O), 533; ν(Sn–N), 462. ^{1}H NMR (300 MHz, DMSO-d_6): δ = 11.34 (s, 1H, NH), 9.53 (s, 2H, CH=N, $^3J(^{119}Sn\text{-}^1H)$ = 37.5 Hz), 8.04-6.76 (m, 20H, Ar-H), 0.75 [s, 12H, Me_2Sn, $^2J(^{119}Sn\text{-}^1H)$ = 88.5 Hz]. ^{119}Sn NMR (111 MHz, DMSO): δ = –292.8

*2.10 Synthesis of [$Ph_4Sn_2L^b$] (**8b**)*

Complex **8b** was synthesized as described for **8a** from H_4L^b (0.148 g, 0.25 mmol), triethylamine (1 mmol) and Ph_2SnCl_2 (0.172 g, 0.5 mmol) after a 4 h reflux. Red plate-like crystals suitable for X-ray crystallography were obtained by slow evaporation of an ethanol solution. Yield: 0.15 g (53%); m.p. 225 °C; Anal. Calcd. for $C_{60}H_{43}N_5O_4Sn_2$: C, 63.47; H, 3.82; N, 6.17 %. Found: C, 63.03; H, 4.06; N, 6.47 %. FT-IR (KBr, cm^{-1}): ν(C=N), 1616, 1600; ν(Sn–O), 521; ν(Sn–N), 448. ^{1}H NMR (250 MHz, DMSO-d_6): δ = 11.24 (s, 1H, NH), 9.57 (s, 2H, CH=N, $^3J(^{119}Sn\text{-}^1H)$ = 47.5 Hz), 8.27–6.49 (m, 40H, Ar-H), ^{119}Sn NMR (111 MHz, DMSO): δ = –407.7.

*2.11. Synthesis of [$Bu_4Sn_2L^b$] (**9b**)*

A solution of H_4L^a (0.148 g, 0.25 mmol) and triethylamine (1 mmol) in ethanol (15 mL) was stirred for 10 min. Bu_2SnCl_2 (0.152 g, 0. 5 mmol) in ethanol (10 mL) was then added. The orange solution was refluxed for 5 h. After this time, a yellow precipitate formed on adding water to the solution. This precipitate was collected and dried in vacuum over $CaCl_2$. Yield: 0.20 g (85%); m.p. 78 °C. Anal. Calcd. for $C_{52}H_{59}N_5O_4Sn_2$: C, 59.17; H, 5.63; N, 6.64 %. Found: C, 58.97; H, 5.71; N, 6.67 %. FT-IR (KBr, cm^{-1}): ν($C–H_{aliphatic}$), 2957-2857; ν(C=N), 1601; ν(Sn–O), 527; ν(Sn–N), 461. ^{1}H NMR (300 MHz, DMSO-d_6): δ = 10.94 (s, 1H, NH), 9.56 (s, 2H, CH=N, $^3J(^{119}Sn\text{-}^1H)$ = 40.0 Hz), 7.96-6.82 (m, 20H, Ar-H), 1.51-1.26 (m, 16H, CH_2CH_2), 1.14-1.03 (m, 8H, CH_2), 0.58 (t, 12H, CH_3, $^3J_{HH}$ = 7.7 Hz). ^{119}Sn NMR (111 MHz, DMSO): δ = –245.7.

2.12. X-ray structure determination

Yellow block like crystals of **7b** and red plates of **8b** were used for data collection. X-ray measurements for both structures were carried out on an Agilent Duo diffractometer using MoK_α radiation ($\lambda = 0.71073$ Å) with data collection, reduction and absorption corrections controlled using *CrysAlisPro* [39] and data were collected at 100(2) K. Data were reduced and multi-scan absorption corrections were applied using *CrysAlisPro* [39]. Both structure was solved by direct methods using *SHELXT* [40] and refined using full-matrix least-squares procedures using *SHELXL-2014/7* [41] and *TITAN2000* [42]. All non-hydrogen atoms were refined anisotropically and all hydrogen atoms bound to carbon were placed in the calculated positions, and their thermal parameters were refined isotropically with U_{eq} = 1.2—1.5 U_{eq}(C). The N—H hydrogen atoms in both molecules were located in difference Fourier maps and their coordinates were refined with U_{eq} = 1.2 U_{eq}(N).

Once all of the non-hydrogen atoms of complex **7b** had been located and refined, several additional high peaks remained in the difference Fourier map that appeared to represent a water molecule and an additional solvent molecule. However assignment and subsequent refinement of these atoms proved difficult with high and increasing displacement parameters suggesting significant disorder in both solvates. However a suitable disorder model could not be found. The contribution to the scattering from these disordered solvates, was therefore removed with the SQUEEZE routine [43] within PLATON [44] and subsequent refinement saw significant improvements to the residuals.

Residuals for **8b** were poor with R1 = 0.0731, which was the best result achieved from data collections on three separate samples. Despite this, the structure solved and refined without difficulty and the relatively poor data is reflected in the uncertainties reported for this structure.

Molecular plots and packing diagrams were drawn using Mercury [45]. Additional metrical data were calculated using PLATON and tabular material was produced using WINGX [46]. Details of the X-ray measurements and crystal data for both complexes are given in Table 1.

2.13. Antibacterial tests and DNA cleavage assay

The antibacterial activity of ligands and complexes at four different concentrations including 2.5, 5, 10 and 20 mg/mL in DMSO were evaluated against *Escherichia coli* ATCC25299, *Pseudomonas aeruginosa* ATCC9027, *Bacillus subtilis* ATCC6633 and *Staphylococcus aureus* ATCC6538 using the Kirby-Bauer standard disc diffusion method [19, 47]. No inhibition zone was found around the discs prepared from these compounds. Hence, none of the tested compounds showed any antibacterial activity.

Drug-DNA interaction was studied simply and sensitively by measuring structural alteration or degradation in circular DNA obtained from either Gram-positive bacteria of *B. subtilis* and *S. aureus* or Gram-negative bacteria of *E. coli* and *P. aeruginosa* on agarose gel electrophoresis. The more potent binding of compounds to DNA provide shorter DNA fragments moving faster on the gel with no retained band in the starting point (loading wells). Accordingly the bacterial DNA was extracted by boiling method [19, 48]. Then a solution of each compound in DMSO (20 mg/mL) was prepared and 10 µL of this solution was mixed with 10 µL of extracted DNA and incubated at 37 ˚C for 2 h. A positive control was prepared by mixing 10 µL of H_2O_2 with 10 µL of DNA and an untreated DNA was used as negative control. These samples then electrophoresed at 100 V for 50 min in a 1% agarose gel containing DNA safe stain. The treated gel was documented under UV irradiation using a UVI-Tec gel documentation system.

2.14. Docking experiments

A double stranded DNA of 12 base pair with AGTCAGTCAGTCAGTC sequence was constructed using ArgusLab software version 4.0.1 (http://www.planaria-software.com/). This structure then equilibrated and optimized at 37 ˚C, pH 7 and 1atomsphere of pressure in Gromacs version 4.6.5 using Amber03 force field. Steep descent algorithm was used for energy minimization and total energy for the system lower than 200 kJ/mol was used as energy minimization criterion. After removing all hetero atoms the optimized structure was used as receptor for docking experiments in Hex version 6.3 (http://hex/loria.fr/). Docking experiments were carried out based on shape and electrostatic mode and default parameters using **6a**, **6b**, **7b** and **8b** with different DNA binding and degrading potency as compounds for docking.

3. Results and discussion

2, 4′-Diphenylamine dicarboxylic acid (**3a**) and 2, 2′-diphenylamine dicarboxylic acid (**3b**) were prepared from the reaction of 2-chlorobenzoic acid (**1**) with 4-aminobenzoic acid (**2a**) and 2-aminobenzoic acid (**2b**), respectively. Then 2-[4-(methoxycarbonyl)phenylamino] benzoic acid methyl ester (**4a**) and 2-[2-(methoxycarbonyl)phenylamino] benzoic acid methyl ester (**4b**) were obtained through esterification of the corresponding diphenylamine dicarboxylic acid, **3a** and **3b**. Hydrazinolysis of the diesters **4a** and **4b** gives 2-[4-(hydrazinecarbonyl) phenylamino] benzoic acid hydrazide (**5a**) and 2-[2-(hydrazinecarbonyl)phenylamino] benzoic acid hydrazide (**5b**), respectively. Condensation of the dihydrazides **5a** and **5b** with 2-hydroxynaphthaldehyde afforded the bis-hydrazones **6a** (H_4L^a) and **6b** (H_4L^b). Figure 2 shows these synthetic pathways.

Bis-aroylhydrazone ligands, H_4L^a and H_4L^b, are isomers with four ionizable protons, two each from the phenol and the amide functions. These ligands each have six potential donor atoms

with two tridentate domains connected by diphenylamine as a linker. The flexibility and tautomerism present in these hydrazones has the potential to allow the ligands or their complexes to adopt different orientations and coordination modes.

Five new binuclear organotin(IV) complexes **7a**, **7b**, **8a, 8b** and **9b** were synthesized by reaction of H_4L^a or H_4L^b with R_2SnCl_2 (R = Me, Ph and *n*-Bu) in the presence of triethylamine as a base in a 1:2:4 ratio. The new complexes were characterized by elemental analysis and IR, ^1H and $^{119}SnNMR$ spectroscopy. The stoichiometry of the complexes was confirmed by the analytical data and integrations in the ^1H NMR spectra. The structures of **7b** and **8b** have also been also confirmed by X-ray crystallography.

3.1. X-ray structures

The structures of **7b** and **8b** were determined by single-crystal X-ray diffraction analysis. Both complexes crystallized in the monoclinic space group C 2/c with eight molecules in a unit cell. Figure 3 shows the molecular structures of **7b** with the structure of **8b** shown in Figure 4. Selected bond lengths and angles are listed in Tables 2 and 3. The structures of both complexes reveal that complexation was preceded by ketone to enol tautomerism accompanied by complete deprotonation of the ligand, Figure 5. The fully deprotonated aroyldihydrazone ligands provide two contiguous ONO tridentate domains each of which coordinate the Sn atoms of two organotin(IV) moieties forming the binuclear complexes. Structural parameters are very similar for the two parts of the complex molecules. This is perhaps to be expected given the symmetrical nature of the $[L^b]^{4-}$ ligand. Each tin center coordinates to the imine nitrogen, phenolic oxygen and enolate oxygen atoms of the $[L^b]^{4-}$ ligands. The two C atoms of the methyl and phenyl substituents of the organotin units increase the coordination numbers of the tin atoms

to five in each case with 5 and 6 membered chelate rings resulting from the coordination of the O2 and N1 or the N1 and O1 atoms respectively. The trigonality index, $\tau = (\alpha - \beta)/60$, was calculated to determine the extent of structural distortion from ideal square pyramidal or trigonal bipyramidal geometries around each tin atom. In this equation, proposed by Reedijk and coworkers [49], α and β are the two largest bond angles around the metal atom in a five-coordinate environment. The τ value for an ideal square pyramidal geometry is zero, while for ideal trigonal bipyramidal geometry it would be unity. In the complex **7b,** the τ value is 0.48 and 0.42 for Sn1 and Sn2 atoms, respectively; therefore both Sn atoms are located in highly distorted square pyramid environment with the imine nitrogen (N1) in the axial position. The imine nitrogen is chosen as axial because none of four donor atoms that make α and β should be placed in apical position. The trigonality index for the Sn1 and Sn2 atoms in complex **8b** are found to be 0.50 and 0.56. This indicates that the coordination geometry around Sn1 in **8b** appears as midway between square-pyramidal and trigonal-bipyramidal. For Sn2, the structure around the metal tends more towards highly distorted trigonal-bipyramidal with the two oxygen atoms are in the axial positions. The rigidity of chelate rings and the large covalent radius of tin(IV) leads to these structural distortions from the ideal geometries [50, 51].

The Sn−N and Sn−O bond distances are considerably shorter than sum of van der Waals radii of the corresponding atoms, 3.85 and 3.80 Å, respectively, although they are very close to the sum of the covalent radii of the elements (Sn−N, 2.15 Å and Sn−O, 2.10 Å) [52, 53]. Therefore, binding in this coordination complex is strong.

A search of the Cambridge Crystallographic Database (version 5.39; updated February 2018) [54] for five-coordinate tin complexes with a C_2SnONO coordination sphere generated an impressive 358 hits. However limiting this search to dimethyl and diphenyl derivatives with a

phenolate–CH=N–N=C–O^- coordination sphere resulted in 36 and 35 hits respectively. Of these only 8 dimethyl and 5 diphenyl derivatives were found to be five coordinate binuclear complexes with the two tin coordination spheres variously bridged alkyl chains [26, 27, 34] and in one instance a benzene ring [25]. These contrast with the diphenylamine link observed here. In only two instances were closely related diphenylmethane bridging systems observed [33].

3.2. Spectroscopic studies

In the spectra of complexes the absence of ν(C=O) and presence of two bands for the ν(C=N) stretching mode, at a lower frequency than the ligand is evidence for the occurrence of a ketone to enol tautomerism prior to coordination of the resulting enolic oxygen and the azomethine nitrogen to tin. New bands were appeared in the ~400-600 cm^{-1} range that may be related to ν(Sn-N) and ν(Sn-O) stretching modes. These further support coordination of the nitrogen and oxygen to the diorganotin(IV) moieties [55-57].

Details of the ^{1}H NMR spectral data of ligands and their complexes in DMSO are presented in the experimental section. H_4L^a is a 2,4′-substituted diphenylamine and so the two segments of the molecule provide slightly different chemical environments, therefore two signals were observed for each of the Ar-OH, –NH–N= and CH=N protons. In contrast, H_4L^b is a symmetrically 2,2′-substituted diphenylamine with chemical equivalence for the equivalent set of protons in solution. In the ^{1}H NMR spectra of complexes, signals due to the four acidic OH protons are absent, suggesting completely deprotonation of the ligand precedes coordination to the tin centers in the enolate form. The ratio of the integrals of the methyl and phenyl resonances

of the organotin moieties to those of the ligands confirms the 2:1 ratio of metal to ligand in the complexes.

In the ^{1}H NMR spectra of **7a** and **8a** two resonances were observed for two imine protons with both signals flanked by satellites due to $^{3}J(^{119}Sn\text{-}H)$ coupling. This confirms the coordination of the two chemically different azomethine nitrogen atoms to the tin(IV) centers. The ^{1}HNMR spectrum of **7a** also clearly shows two singlets for the resonances of the Me_2Sn protons confirming that the complex is binuclear with discrete environments for the chemically different dimethyltin moieties. A singlet resonance attributable to the two imine protons appears in the spectrum of the more symmetrical H_4L^b. This is shifted slightly downfield and accompanied by ^{119}Sn satellites in the spectra of **7b** and **8b** confirming that the environments of the coordinated tin(IV) centers are magnetically equivalent a fact further indicated by the appearance of the 12 methyl protons of the $SnMe_2$ groups of **7b** as a singlet resonance . The coupling constants, $^{2}J(^{119}Sn\text{-}^{1}H)$, in of the methyl groups in the dimethyltin complexes, **7a** (88.3 Hz) and **7b** (88.5 Hz), are larger than those for Me_2SnCl_2 (68.7 Hz) due to the increased coordination numbers of the tin centers. Substitution of this coupling constant into the Lockhart-Manders equation [58], $\theta = 0.016|^{2}J|^{2} - 1.32|^{2}J| + 133.4$, gives values of 141.6° and 141.9° for the CH_3-Sn-CH_3 angles of **7a** and **7b**, respectively, in DMSO solution. This value for **7b** is different from the value obtained from X-ray data in solid state. The discrepancy is doubtless due to variations between the solid state and solution structures. The $^{2}J(^{119}Sn\text{-}^{1}H)$ value for Sn–CH_2 in butyl complex cannot be extracted from the spectrum because of the complexity of the methylene multiplets. All complexes show multiplets at 8.4–7.0 ppm for aromatic protons of ligand. The phenyl protons of the Ph_2Sn groups in **8a** and **8b** also appear in this range. These signals cannot be carefully assigned due to significant overlap of the multiplets.

The ^{119}SnNMR spectra of **7a** and **8a** show two sharp signals close together because of the chemical environments of two tin centers in these complexes, while distinguishable, are only slightly different. ^{119}Sn resonances for two tin centers in **7a** appear at –208.2 and –233.6 and at –399.6, –420.4 ppm for **8a**. All these chemical shifts are at significantly lower frequencies in comparison to the Me_2SnCl_2 (+137 ppm) and Ph_2SnCl_2 (-32 ppm) starting materials [16]. This is again a result of the increase in the coordination number at the tin centers. Based on the empirical chemical shift ranges observed for a variety of related organotin compounds, the coordination number of the tin atoms in both complexes is five. The appearance of only one sharp singlet in the ^{119}Sn NMR spectra of **7b**-**9b** indicates similar environments for two tin centers in all of these complexes as expected. The values of these chemical shifts, –292.8, –407.7 and –245.7 ppm for **7b, 8b** and **9b**, respectively, are again indicative of a coordination number of five for both tin centers in all of the complexes. It is generally found that the chemical shifts for diphenyltin complexes appear at higher field due to anisotropic shielding effects and possible π-interactions [28]. Signals are also found to appear at lower frequencies in coordinating solvents such as DMSO [59].

3.3 Antibacterial activity and DNA cleavage

Based on antibacterial activity assessment in standard Kirby- Bauer disc diffusion method, none of the tested ligands or their complexes were found to inhibit bacterial growth, i.e., no inhibition zone was performed. These observations may be attributed to impermeability of bacterial cell wall against these compounds and the probable absence of carrier system for active transport of these large chemicals across cell wall and bilayer cytoplasmic membrane. On the other hand, this finding reveals that there isn't any target site for these compounds on bacterial cell wall. So,

these compounds can't interact with any of enzymes involved in cell wall synthesis and growth, carrier proteins, porins of outer membrane and enzymes of electron transport system [60-63].

As indicated in Figure 6, the ligands (**6a** and **6b)** have completely changed DNA structures for all strains used in this study and in comparison **6a** behave more potently than **6b**, the character should rely on its more effective interaction. This Figure also shows that among organotin complexes **7a** and to lesser extent **7b**, reveals low degrees of DNA structural alterations with week bands retained in loading wells. The rest tin complexes of **8a**, **8b** and **9b** show no significant interaction with DNA due to unaffected bands in loading wells. To see what happen in these experiments and to understand underling mechanism we turned to modeling and docking experiment.

3.4 Molecular Modeling and Docking

DNA cleavage assays have shown that both free ligands of **6a** and **6b** and also tin complex of **7a** and **7b** show activity in this context. In addition to **6a**, **6b** and **7b**, we selected **8b** as inactive complex for docking experiments and comparison.

It is important to know that the ability of a compound to interact with DNA and perturb its native structure has potential applications in cancer therapy. DNA binding compounds may bind via their planar aromatic moiety and insertion between base pairs of DNA, the process called intercalation and by this way they facilitate DNA degradation [64]. Double stranded DNA in its three dimensional structure contain a wide and shallow binding pocket called major groove which is suitable for binding of large molecules as regulatory protein and not small molecules as our chemicals. There is another narrow and deep binding pocket which is more effective for drug or chemical compound binding called minor groove [65, 66]. Therefore it seems logic that more

effective compounds in our experiment should bind to DNA through minor groove and the more binding energy calculated for each compound should correlate with more degrading behavior.

As indicated in method section and in order to perform well designed docking experiments we constructed a DNA molecule with 12bp with uniform distribution of nucleotide to prevent sequence dependent binding energy for different compounds. This artificial DNA should be converted to an equilibrated minimized structure at native like conditions of neutral pH, 37 ˚C, 0.1 M salinity and 1 atmosphere of pressure. The structure of compounds used in these experiments including **6a**, **6b**, **7b** and **8b** were minimized in ArgusLAb and used for docking. The total of 100 docking conformations or poses for each compound were saved and analyzed for comparison. The binding energy of 100 poses for compounds were analyze in SPSS and one way ANOVA and paired-sample T-test to compare their average. The average energies obtained for **6a, 6b, 7b** and **8b** were calculated as -340.36±6.0, -305.26±5.8 -309.89±2.36 and -274.37±2.6 kJ/mol, respectively (at p-value<0.001 level). These energies are in agreement with DNA cleavage potency sequence of **6a>7b>6b>8b**, the more potent binding compound cause the more degrading ability. Graphical survey of the binding conformations for our compounds (Figure 7) illustrates that among these compounds, **6a** (Figure 7A) has more linear structure and fits better to double stranded DNA and more importantly binds DNA through its minor groove. This interprets more potent binding energy and more DNA cleavage ability of **6a** in our observations. Compound **6b** (Figure 7B) due to its curved and globular structure (contrast to **6a**) could not bind to minor groove of DNA and obliged to interact via major groove. As indicated earlier this contact is not efficient for binding, so the binding energy of **7b** exceeds that's of **6b**. Indeed **7b** as shown in Figure 7C interact with DNA by inserting one of its bicyclic moieties inside minor groove to stacks with DNA base pairs. Substitution of phenyl groups instead of

methyl groups in **7b** leads to **8b** complex. Figure 8 illustrates clearly that the four larger phenyl groups by occupying surrounding space of **8b** prevent bicyclic moieties of the molecule interact with minor groove part of DNA and hence this compound arbitrary bind to DNA via major groove with architecture not compatible with effective stacking with DNA base pairs (Figure 7D). Hence the mode of interaction suggested by molecular docking for our compounds seems to adapt our experimental findings.

4. Conclusion

Both symmetric and unsymmetric bis-hydrazones used in this work are completely deprotonated and coordinated to two diorganotin moiety through two ONO tridentate binding pocket. Therefore dinulear organtin(IV) complexes with diphenylamine as linker were formed in which coordination number of each tin will be five. Despite the lack of antibacterial activity of the synthesized ligands and complexes, probably because of impermeability of bacterial cell walls, DNA degradation and complimentary docking experiments reveal that ligands as well as dimethyltin complexes show prominent DNA binding ability. These compounds that bind through minor groove of DNA are appropriate to study for their anti cancer effects, taking in to account that the impermeability of bacterial cell wall does not means that these compounds did not pass human cell membranes, because cell membrane contain miscellaneous mechanisms for transportation.

Acknowledgment

Support of this work by Shahid Chamran University of Ahvaz, Ahvaz, Iran (Grant No. 1396) is gratefully acknowledged. We also thank the University of Otago for purchase of the diffractometer and the Chemistry Department, University of Otago for support of the work of JS.

Appendix A. Supplementary material

CCDC 1824768 and 1824769 contains the supplementary crystallographic data for **7b** and **8b**, respectively. These data can be obtained free of charge via http://www.ccdc.cam.ac.uk/conts/retrieving.html, or from the Cambridge Crystallographic Data Centre, 12 Union Road, Cambridge CB2 1EZ, UK; fax: +44 1223 336 033; or e-mail: deposit@ccdc.cam.ac.uk.

References

[1] A.-M. Stadler, J. Harrowfield, Inorg. Chim. Acta, 362 (2009) 4298-4314.

[2] D.P. Singh, R. Dwivedi, A.K. Singh, B. Koch, P. Singh, V.P. Singh, Sens. Actuators, B, 238 (2017) 128-137.

[3] I. Syiemlieh, A. Kumar, S.D. Kurbah, R.A. Lal, J. Mol. Struct., 1166 (2018) 252-261.

[4] L.D. Popov, A.N. Morozov, I.N. Shcherbakov, Y.P. Tupolova, V.V. Lukov, V.A. Kogan, Russ. Chem. Rev., 78 (2009) 643-658.

[5] G.K. Patra, R. Chandra, A. Ghorai, K.K. Shrivas, Inorg. Chim. Acta, 462 (2017) 315-322.

[6] H. Adams, D.E. Fenton, G. Minardi, E. Mura, A.M. Pistuddi, C. Solinas, Inorg. Chem. Commun., 3 (2000) 24-28.

[7] P. Zabierowski, M. Oszajca, M. Hodorowicz, D. Matoga, Polyhedron, 121 (2017) 25-32.

[8] T.S. Abedin, L.K. Thompson, D.O. Miller, E. Krupicka, Chem. Commun., (2003) 708-709.

[9] S.K. Dey, T.S. Abedin, L.N. Dawe, S.S. Tandon, J.L. Collins, L.K. Thompson, A.V. Postnikov, M.S. Alam, P. Müller, Inorg. Chem., 46 (2007) 7767-7781.

[10] S. Naskar, D. Mishra, S.K. Chattopadhyay, M. Corbella, A.J. Blake, Dalton Trans., (2005) 2428-2435.

[11] K. Anđelković, M.R. Milenković, A. Pevec, I. Turel, I.Z. Matić, M. Vujčić, D. Sladić, D. Radanović, G. Brađan, S. Belošević, B. Čobeljić, J. Inorg. Biochem., 174 (2017) 137-149.

[12] S.D. Kurbah, A. Kumar, I. Syiemlieh, M. Asthana, R.A. Lal, Inorg. Chem. Comm., 86 (2017) 39-43.

[13] M. Gielen, Tin chemistry: fundamentals, frontiers, and applications, John Wiley & Sons, 2008.

[14] A. Tarassoli, T. Sedaghat, in: R.P. Irwin (Ed.) Organometallic Chemistry Research Perspectives, Nova Science Publishers, New York, 2007, pp. 221-248.

[15] M. Gielen, E.R. Tiekink, Metallotherapeutic drugs and metal-based diagnostic agents: the use of metals in medicine, John Wiley & Sons, 2005.

[16] A.G. Davies, Organotin chemistry, John Wiley & Sons, 2006.

[17] P.J. Smith, Chemistry of tin, Springer Science & Business Media, 2012.

[18] K. Liu, H. Yan, G. Chang, Z. Li, M. Niu, M. Hong, Inorg. Chim. Acta, 464 (2017) 137-146.

[19] T. Sedaghat, Y. Ebrahimi, L. Carlucci, D.M. Proserpio, V. Nobakht, H. Motamedi, M.R. Dayer, J. Organomet. Chem., 794 (2015) 223-230.

[20] S. Kumar, M. Nath, J. Organomet. Chem., 856 (2018) 87-99.

[21] C. González-García, A. Mata, F. Zani, M.A. Mendiola, E. López-Torres, J. Inorg. Biochem., 163 (2016) 118-130.

[22] Y. Yang, M. Hong, L. Xu, J. Cui, G. Chang, D. Li, C.-z. Li, J. Organomet. Chem., 804 (2016) 48-58.

[23] Z. Ansari-Asl, T. Sedaghat, A. Tarassoli, H. Motamedi, E. Hoveizi, Phosphorus, Sulfur Silicon Relat. Elem, 192 (2017) 538-543.

[24] M.P. Degaonkar, V.G. Puranik, S.S. Tavale, S. Gopinathan, C. Gopinathan, B. Chem. Soc. Jpn, 67 (1994) 1797-1801.

[25] H.-d. Yin, J.-c. Cui, Y.-l. Qiao, Polyhedron, 27 (2008) 2157-2166.

[26] T. Sedaghat, M. Aminian, G. Bruno, H. Amiri Rudbari, J. Organomet. Chem., 737 (2013) 26-31.

[27] T. Sedaghat, M. Aminian, H. Amiri Rudbari, G. Bruno, J. Organomet. Chem., 754 (2014) 26-31.

[28] S. Shujah, N. Muhammad, A. Shah, S. Ali, A. Meetsma, Z. Hussain, J. Organomet. Chem., 759 (2014) 19-26.

[29] D.K. Dey, S.P. Dey, N.K. Karan, A. Lyčka, G.M. Rosair, J. Organomet. Chem., 749 (2014) 320-326.

[30] T. Sedaghat, M. Aminian, M. Azarkish, Phosphorus, Sulfur, and Silicon and the Related Elements, 190 (2015) 352-359.

[31] H. Zafarian, T. Sedaghat, H. Motamedi, H.A. Rudbari, J. Organomet. Chem., 825 (2016) 25-32.

[32] S. Kumar, M. Nath, J. Organomet. Chem., 853 (2017) 113-121.

[33] H. Zafarian, T. Sedaghat, H. Motamedi, D. Trzybiński, K. Woźniak, J. Organomet. Chem., 853 (2017) 184-192.

[34] H. Ullah, B. Twamley, A. Waseem, M. Khawar Rauf, M.N. Tahir, J.A. Platts, R.J. Baker, Cryst. Growth Des., 17 (2017) 4021-4027.

[35] T. Shimizu, Y. Fujiwara, T. Osawa, T. Sakai, K. Kubo, K. Kubo, T. Nishitoba, K. Kimura, T. Senga, H. Murooka, Bioorg. Med. Chem. Lett., 14 (2004) 875-879.

[36] S.M. Abou-Seri, Eur. J. Med. Chem., 45 (2010) 4113-4121.

[37] A.A.H.M. Eissa, G.A.E.-H. Soliman, M.H. Khataibeh, Chem. Pharm. Bull., 60 (2012) 1290-1300.

[38] I.B. Taraporewala, J.M. Kauffman, J. Pharm. Sci., 79 (1990) 173-178.

[39] P. CrysAlis, Agilent Technologies Ltd: Yarnton, 2013.

[40] G. Sheldrick, Acta Cryst. A, 71 (2015) 3-8.

[41] G. Sheldrick, Acta Cryst. C, 71 (2015) 3-8.

[42] K. Hunter, J. Simpson, TITAN2000: A molecular graphics program to aid structure solution and refinement with the SHELX suite of programs, 1999.

[43] A. Spek, Acta Cryst. C, 71 (2015) 9-18.

[44] A. Spek, Acta Cryst. D, 65 (2009) 148-155.

[45] C.F. Macrae, I.J. Bruno, J.A. Chisholm, P.R. Edgington, P. McCabe, E. Pidcock, L. Rodriguez-Monge, R. Taylor, J.v. Streek, P.A. Wood, J. Appl. Cryst., 41 (2008) 466-470.

[46] L.J. Farrugia, J. Appl. Cryst., 30 (1997) 565-565.

[47] J. Vandepitte, J. Verhaegen, K. Engbaek, P. Rohner, P. Piot, C. Heuck, Basic laboratory procedures in clinical bacteriology, World Health Organization, 2003.

[48] J. Sambrook, E.F. Fritsch, T. Maniatis, Molecular cloning, Cold spring harbor laboratory press New York, 1989.

[49] A.W. Addison, T.N. Rao, J. Reedijk, J. van Rijn, G.C. Verschoor, J. Chem. Soc., Dalton Trans., (1984) 1349-1356.

[50] C. Pettinari, F. Marchetti, R. Pettinari, D. Martini, A. Drozdov, S. Troyanov, Inorg. Chim. Acta, 325 (2001) 103-114.

[51] S. Öztaş, E. Şahin, N. Ancın, S. Ide, M. Tüzün, J. Mol. Struct., 705 (2004) 107-112.

[52] B. Cordero, V. Gómez, A.E. Platero-Prats, M. Revés, J. Echeverría, E. Cremades, F. Barragán, S. Alvarez, Dalton Trans., (2008) 2832-2838.

[53] S. Batsanov, Inorg. Materials, 37 (2001) 871-885.

[54] C.R. Groom, I.J. Bruno, M.P. Lightfoot, S.C. Ward, Acta Cryst. B, 72 (2016) 171-179.

[55] T. Sedaghat, M. Naseh, G. Bruno, H. Amiri Rudbari, H. Motamedi, J. Mol. Struct., 1026 (2012) 44-50.

[56] B. Yearwood, S. Parkin, D.A. Atwood, Inorg. Chim. Acta, 333 (2002) 124-131.

[57] T. Sedaghat, M. Yousefi, G. Bruno, H. Amiri Rudbari, H. Motamedi, V. Nobakht, Polyhedron, 79 (2014) 88-96.

[58] T.P. Lockhart, W.F. Manders, Inorg. Chem., 25 (1986) 892-895.

[59] L.S. Zamudio-Rivera, R. George-Tellez, G. López-Mendoza, A. Morales-Pacheco, E. Flores, H. Höpfl, V. Barba, F.J. Fernández, N. Cabirol, H.I. Beltrán, Inorg. Chem., 44 (2005) 5370-5378.

[60] E. Padan, Encyclopedia of Life Sciences (ELS). John Wiley-Sons Ltd, Chichester, (2009).

[61] H. Bajaj, S. Acosta Gutierrez, I. Bodrenko, G. Malloci, M.A. Scorciapino, M. Winterhalter, M. Ceccarelli, ACS nano, 11 (2017) 5465-5473.

[62] H. Nikaido, Mol. Microbiol., 6 (1992) 435-442.

[63] G.J. Mitchell, K. Wiesenfeld, D.C. Nelson, J.S. Weitz, J. Roy. Soc Interface, 10 (2013) 20120892.

[64] A. Mukherjee, W.D. Sasikala, Drug–DNA intercalation: from discovery to the molecular mechanism, in: Advances in protein chemistry and structural biology, Elsevier, 2013, pp. 1-62.

[65] C.T. Winston, D.L. Boger, Chem. Biol., 11 (2004) 1607-1617.

[66] S. Neidle, Nat. Prod. Rep., 18 (2001) 291-309.

Table 1 Crystallographic and structure refinement data for **7b and 8b**

	7b	**8b**
Empirical formula	$C_{40}H_{33}N_5O_4Sn_2$	$C_{60}H_{42}N_5O_4Sn_2$
Formula weight	885.09	1134.36
T (K)	100(2)	100(2)
Wavelength, λ (Å)	1.54184	1.54184
Crystal system	Monoclinic	Monoclinic
Space group	C 2/c	C 2/c
Crystal size (mm^3)	0.18 × 0.11 × 0.09	0.21 × 0.08 × 0.08
a (Å)	24.8269(4)	28.8935(19)
b (Å)	11.5856(3)	8.7165(5)
c (Å)	26.5907(4)	40.270(3)
α (˚)	90	90
β (˚)	102.587(2)	106.740(7)
γ (˚)	90	90
V ($Å^3$)	7464.6(3)	9712.2(11)
Z	8	8
F(000)	3520	4552
Index ranges	-25≤ h ≤25	-35≤ h ≤35
	-11≤ k ≤ 8	-10≤ k ≤10
	-26≤ l ≤ 26	-49≤ l ≤ 49
Reflections collected	19011	44706
Independent reflections	3833	9650 [R(int) = 0.1078]
Completeness to theta = 67.684 ˚	100 %	100 %
Absorption correction	Multi-scan	
Max. and min. transmission	1.0000 and 0.69429	1.0000 and 0.57769
Refinement method	Full-matrix least squares on F^2	
Data / restraints / parameters	3833/0/467	9650 / 72 / 631
Goodness-of-fit on F^2	0.882	1.054
Final R indices [I>2sigma(I)]	R1 = 0.0211, wR2 = 0.0540	R1 = 0.0731, wR2 = 0.1820
R indices (all data)	R1 = 0.0225, wR2 = 0.0549	R1 = 0.0888, wR2 = 0.1935
Largest diff. peak and hole	0.307 and -0.543	2.833 and -2.042 $e.Å^{-3}$

Table 2. Bond lengths [Å] and angles [°] for complex **7b**

Sn1–O1	2.095(2)	Sn2–O1′	2.097(3)
Sn1–O2	2.132(2)	Sn2–O2′	2.144(2)
Sn1–C19	2.110(4)	Sn2–C19′	2.103(4)
Sn1–C20	2.106(4)	Sn2–C20′	2.099(4)
Sn1–N1	2.148(3)	Sn2–N1′	2.141(4)
C12–O2	1.306(5)	C12′–O2′	1.305(5)
C11–N1	1.303(5)	C11′–N1′	1.305(5)
N1–N2	1.403(4)	N1′–N2′	1.400(4)
N2–C12	1.307(5)	N2′–C12	1.299(5)
C2–O1	1.316(5)	C2′–O1′	1.306(5)
C14–N3	1.382(5)	C14′–N3	1.381(5)
O1–Sn1-O2	154.04(12)	O1′–Sn2-O2′	155.14(12)
O1–Sn1–C19	94.70(13)	O1′–Sn2–C19′	97.41(16)
O1–Sn1–C20	97.26(13)	O1′–Sn2–C20′	93.90(16)
O2–Sn1–C19	93.04(13)	O2′–Sn2–C19′	95.33(15)
O2–Sn1–C20	98.30(13)	O2′–Sn2–C20′	94.17(15)
O1–Sn1–N1	81.69(11)	O1′–Sn2–N1′	81.26(12)
C19–Sn1–C20	125.44(17)	C19′–Sn2–C20′	129.9(2)
O2–Sn1–N1	73.66(11)	O2′–Sn2–N1′	73.94(12)
N1–Sn1–C19	125.42(14)	N1′–Sn2–C19′	116.85(17)
N1–Sn1–C20	108.96(14)	N1′–Sn2–C20′	113.07(15)
N2–C12–O2–Sn1	1.7(4)	N2′–C12′–O2′–Sn2	-4.9(5)
C1–C2–O1–Sn1	8.6(5)	C1′–C2′–O1′–Sn2	-15.1(6)
C1–C11–N1–Sn1	-2.1(5)	C1′–C11′–N1′–Sn2	4.4(6)
Sn1–N1–N2–C12	4.3(4)	Sn2–N1′–N2′–C12′	8.2(4)
N1–N2– C12–O2	-4.0(5)	N1′–N2′– C12′–O2′	-2.1(5)
C2–C1–C11–N1	-3.4(6)	C2′–C1′–C11′–N1′	8.5(6)

Table 3. Bond lengths [Å] and angles [°] for complex **8b**

Sn1–O1	2.084(6)	Sn2–O1′	2.082(6)
Sn1–O2	2.110(6)	Sn2–O2′	2.126(5)
Sn1–C19	2.121(7)	Sn2–C19′	2.118(8)
Sn1–C25	2.114(9)	Sn2–C25′	2.118(9)
Sn1–N1	2.140(6)	Sn2–N1′	2.141(4)
C12–O2	1.307(9)	C12′–O2′	1.313(9)
C11–N1	1.300(10)	C11′–N1′	1.295(9)
N1–N2	1.401(9)	N1′–N2′	1.394(8)
N2–C12	1.315(10)	N2′–C12	1.303(10)
C2–O1	1.312(11)	C2′–O1′	1.299(9)
C14–N3	1.402(10)	C14′–N3	1.299(9)
O1–Sn1-O2	155.5(2)	O1′–Sn2-O2′	155.2(2)
O1–Sn1–C19	97.1(3)	O1′–Sn2–C19′	96.9(3)
O1–Sn1–C25	93.3(3)	O1′–Sn2–C25′	95.2(3)
O2–Sn1–C19	98.0(3)	O2′–Sn2–C19′	93.4(3)
O2–Sn1–C25	94.2(3)	O2′–Sn2–C25′	98.5(3)
O1–Sn1–N1	82.6(2)	O1′–Sn2–N1′	82.1(2)
C19–Sn1–C25	123.5(3)	C19′–Sn2–C25′	121.5(3)
O2–Sn1–N1	74.1(2)	O2′–Sn2–N1′	73.3(2)
N1–Sn1–C19	110.8(3)	N1′–Sn2–C19′	121.6(3)
N1–Sn1–C25	125.6(3)	N1′–Sn2–C25′	116.7(3)
N2–C12–O2–Sn1	-11.0(9)	N2′–C12′–O2′–Sn2	-13.0(9)
C1–C2–O1–Sn1	-1.6(12)	C1′–C2′–O1′–Sn2	-21.0(12)
C1–C11–N1–Sn1	13.1(12)	C1′–C11′–N1′–Sn2	11.3(11)
Sn1–N1–N2–C12	5.8(8)	Sn2–N1′–N2′–C12′	12.0(8)
N1–N2– C12–O2	3.5(10)	N1′–N2′– C12′–O2′	0.8(10)
C2–C1–C11–N1	5.0(12)	C2′–C1′–C11′–N1′	9.5(12)

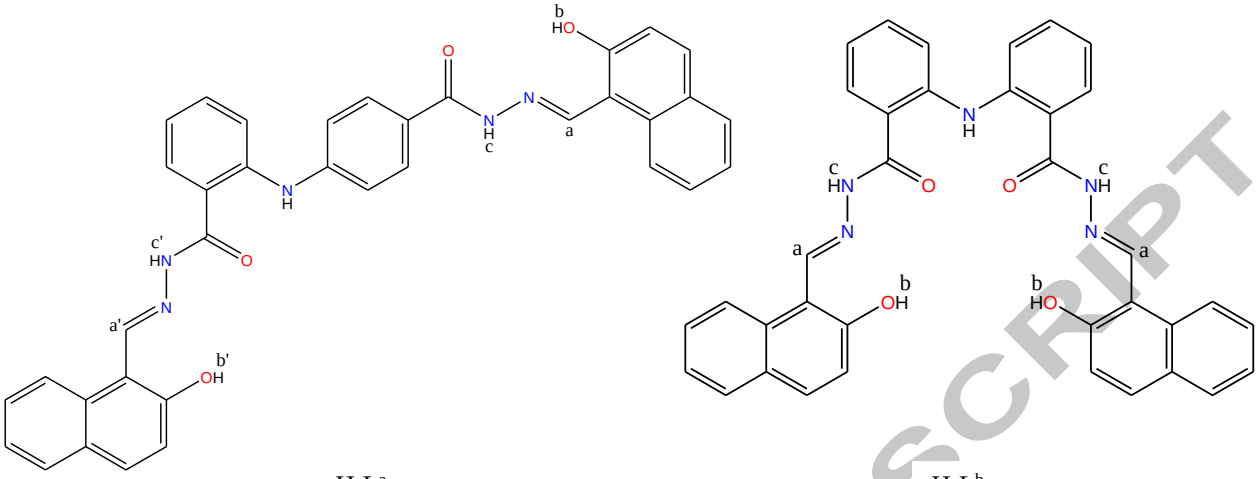

Figure 1. Structure of dihydrazone ligands, H_4L^a (**6a**) and H_4L^b (**6b**) with lettering for ^1H NMR assignments

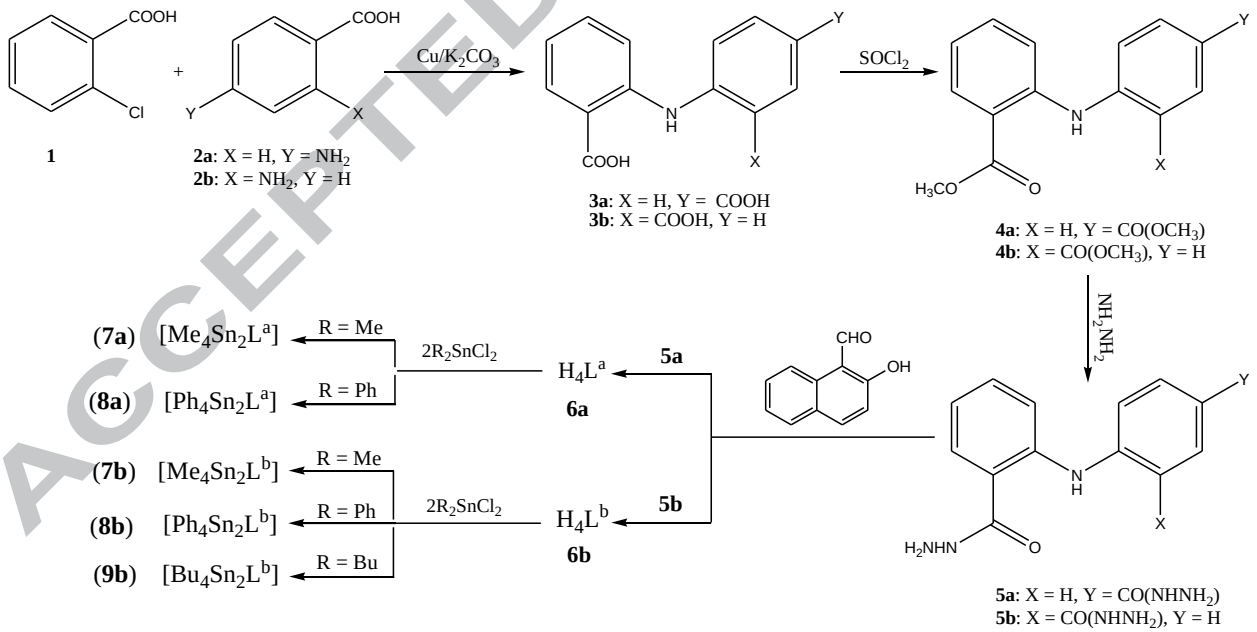

Figure 2. Synthetic pathway to the ligands and their complexes

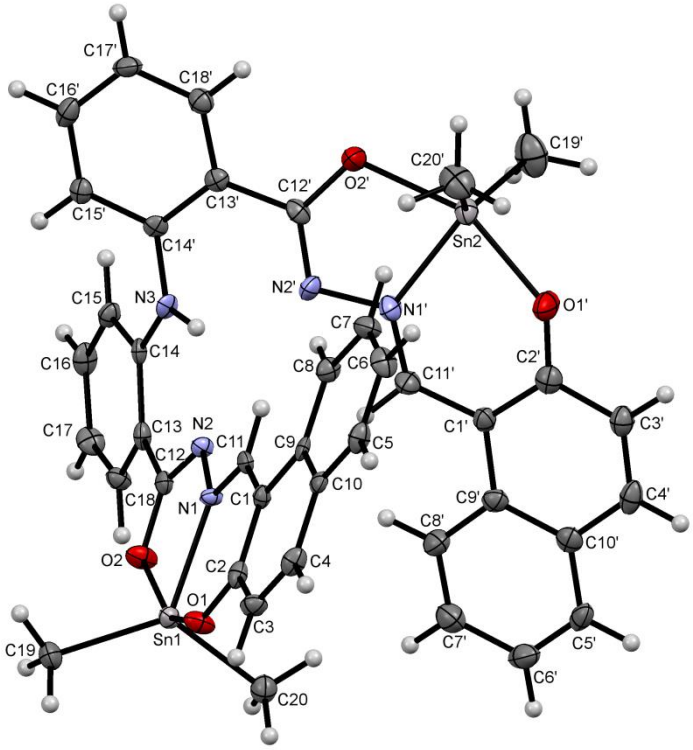

Figure 3. The structure of complex **7b**.

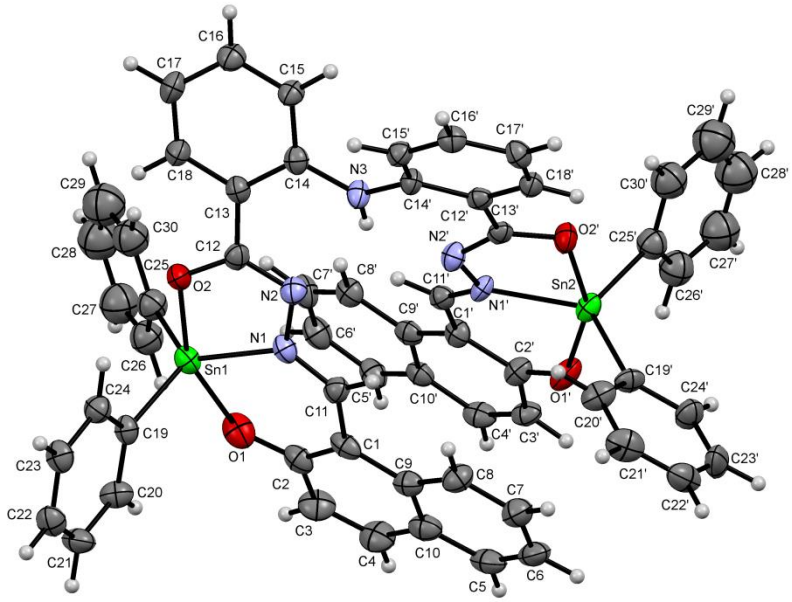

Figure 4. The structure of complex **8b**.

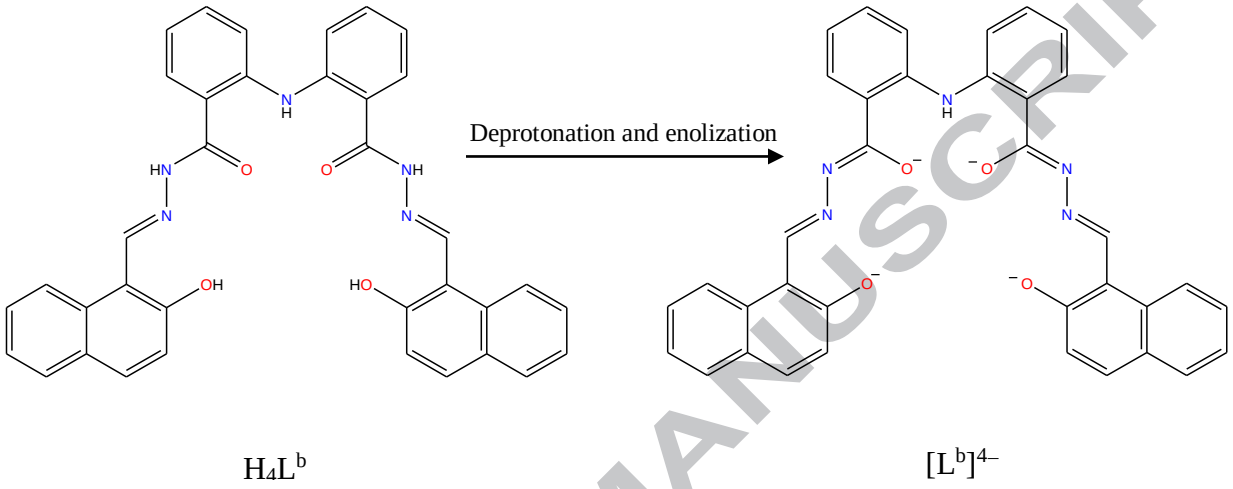

Figure 5. Enolization and deprotonation of ligand H_4L^b prior to complex formation.

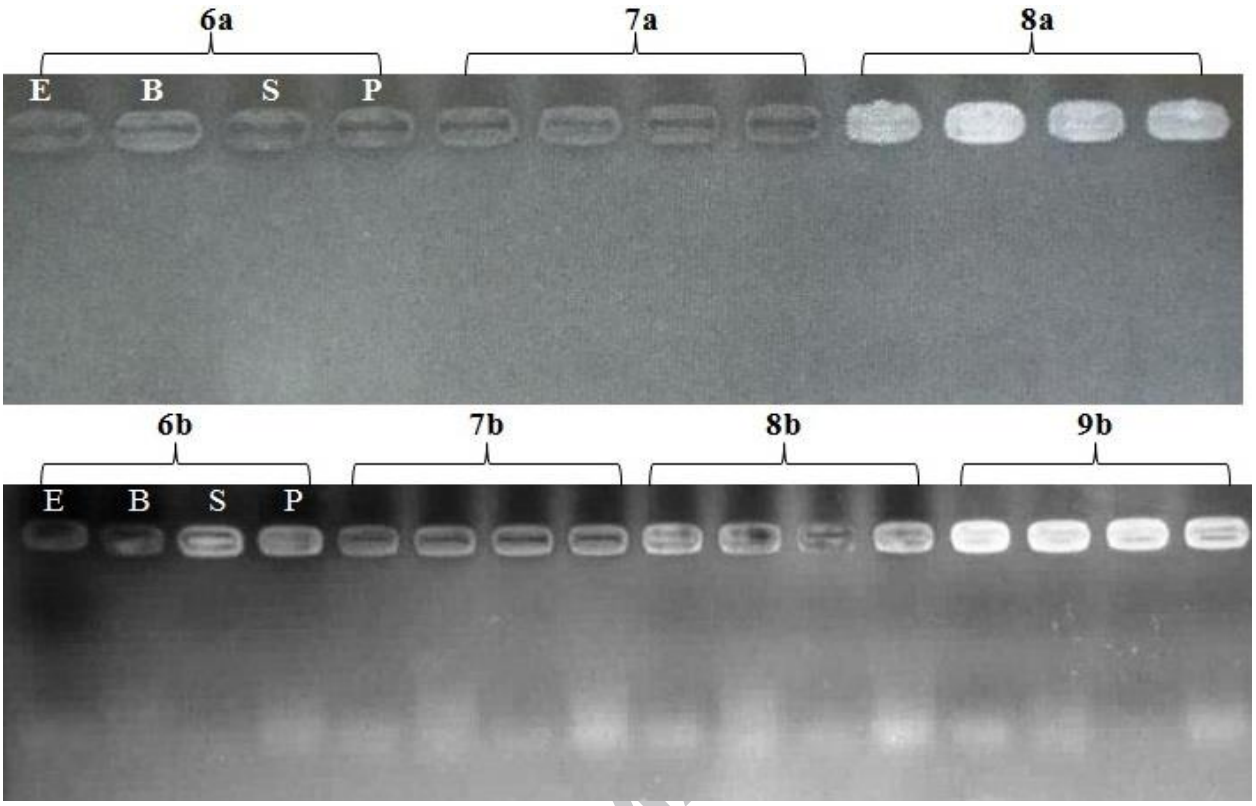

Figure 6. The electrophotogram for the cleavage activity of ligands and their complexes on the isolated DNA of bacteria: E = *E. coli*, B = *B. subtilis*, S = *S. aureus*, P = *P. aeruginosa*

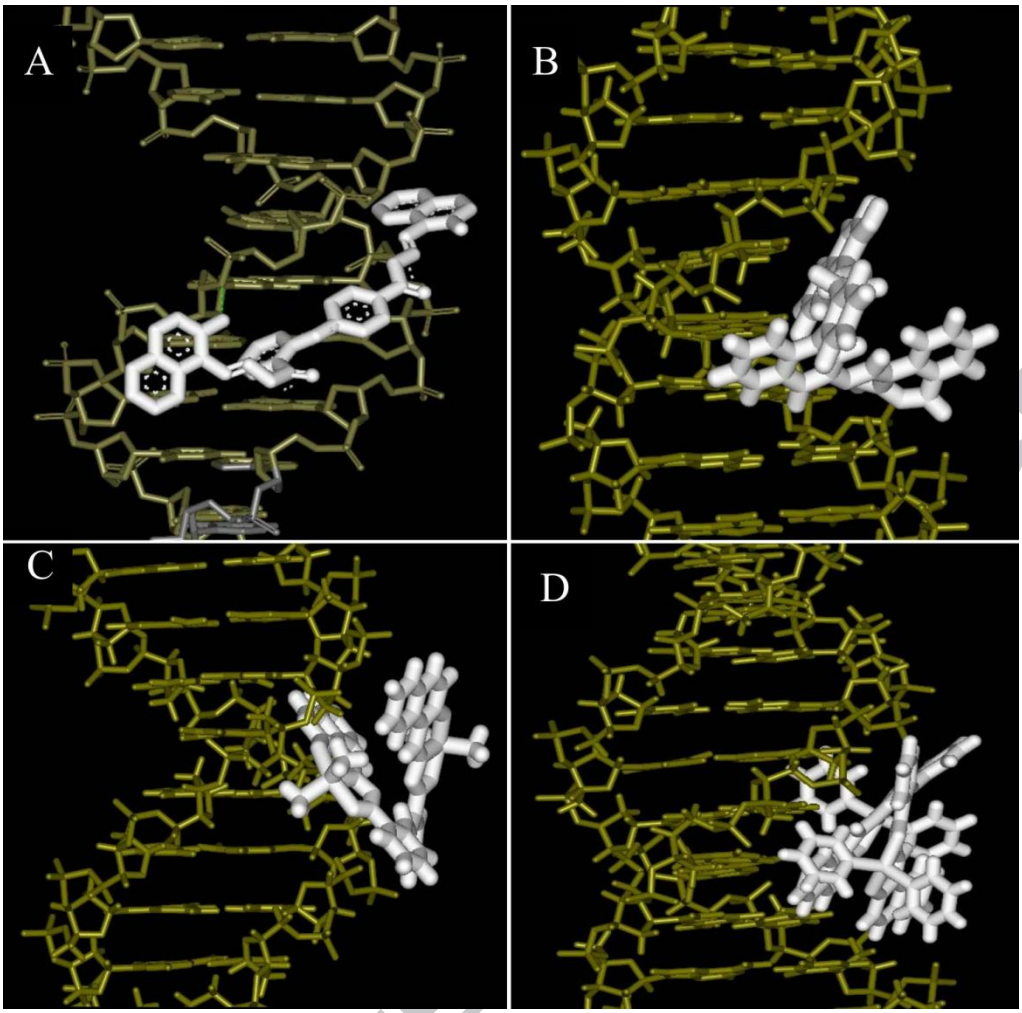

Figure 7. Docking results for **6a** (A), **6b** (B), **7b** (C) and **8b** (D) extracted for Hex software. The compounds that interact with DNA are shown in white color.

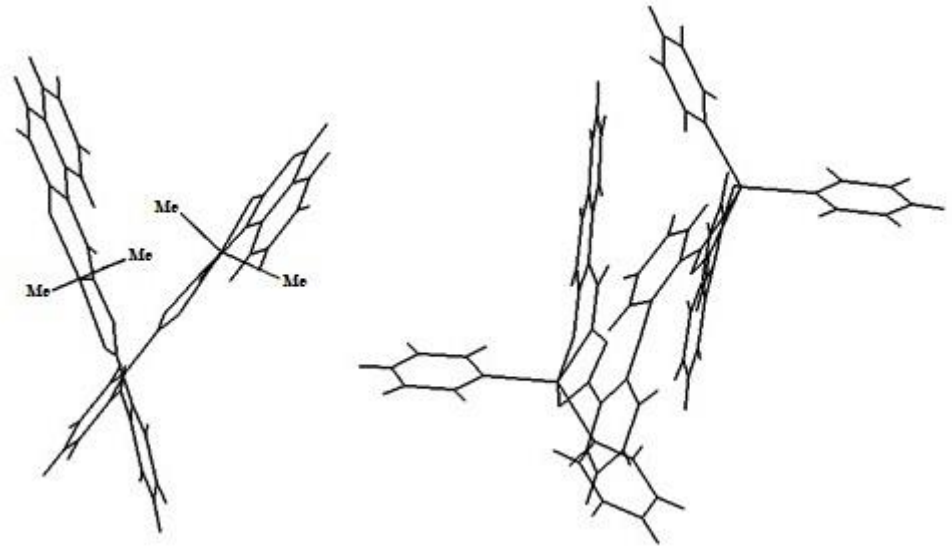

Figure 8. A simplified representation of the surrounding space of **7b** (left) and **8b** (right)

Graphical abstract

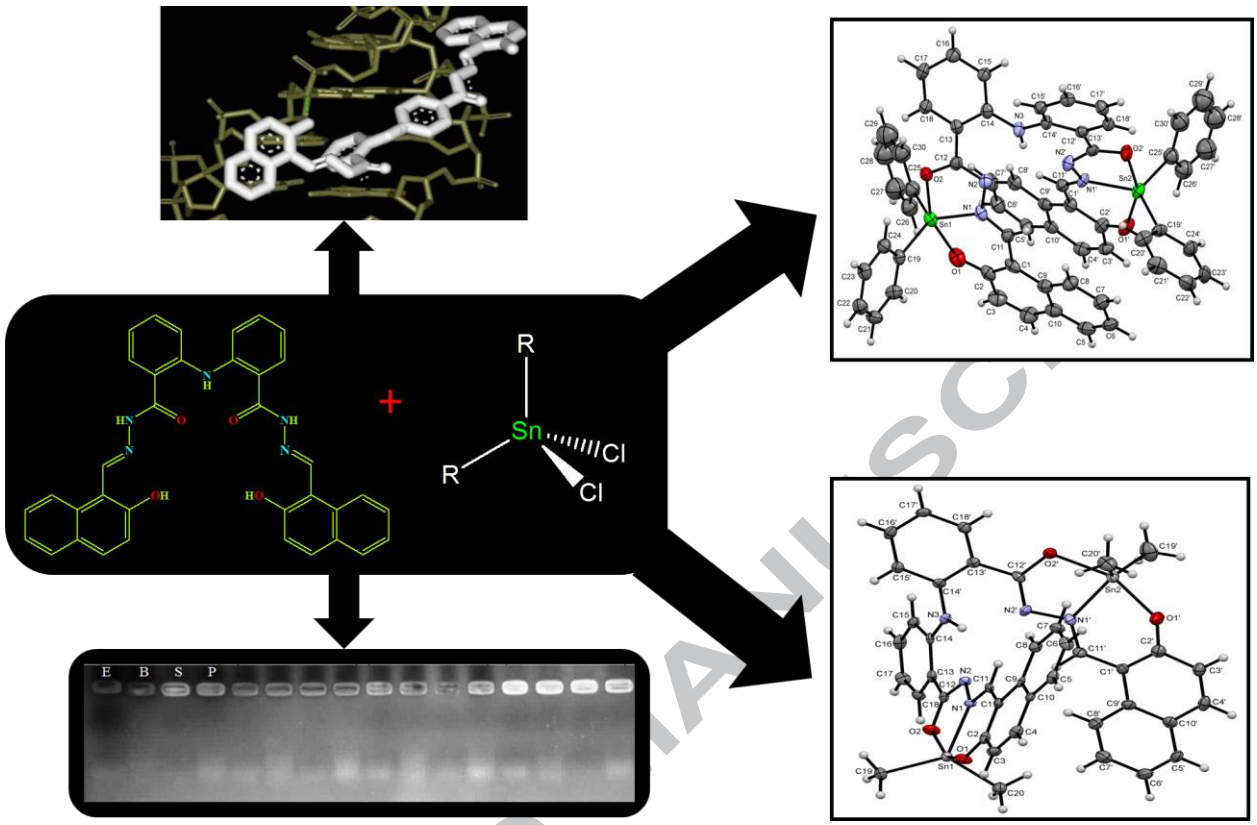

Five new dinuclear organotin(IV) complexes have been synthesized and investigated by spectral methods and X-ray crystallography. Biological activity and molecular docking of ligands and complexes have been also investigated.